A 6-/12-dB Back-off Multi-Mode GaN MMIC Doherty Power Amplifier for 5G Applications

Hansik Oh[#1], Woojin Choi[$], Jaekyung Shin[$], Yifei Chen[$], Hyunuk Kang[#], Young Yun Woo[#], Youngoo Yang[$2]
[#]Samsung Electronics, Republic of Korea
[$]Department of Electrical and Computer Engineering, Sungkyunkwan University, Republic of Korea
[1]hansik.oh@samsung.com, [2]yang09@skku.edu

***Abstract* — This paper presents a multi-mode Doherty power amplifier (M-DPA) MMIC. By arranging the turn-on transitions of four parallel amplifiers, two carrier and two peaking amplifiers (2C2P) mode for 6 dB output power back-off (OBO) or one carrier and three peaking amplifiers (1C3P) mode for 12 dB OBO can be configured. The performances between efficiency and gain can be balanced according to the selected mode. For verification, the M-DPA MMIC was implemented using a 0.25 μm GaN-HEMT process for 5G NR applications (3.3-3.6 GHz band). At 3.55 GHz, the drain efficiencies (DEs) of 37.7 and 33.8% and power gains of 8.3 and 6.4 dB were obtained for the 2C2P mode at 37.0 dBm and for the 1C3P mode at 31.0 dBm, respectively.**

***Keywords* — GaN MMIC, Doherty power amplifier, multi-mode amplifier, multi-mode load modulation, 5G new radio.**

I. Introduction

To increase the efficiency of power amplifiers (PAs) especially at a large output power back-off (OBO) level, various structures based on load modulation have been proposed [1]-[12]. Doherty power amplifiers (DPAs) can improve the efficiency for the modulated signals with a high data rate and large peak-to-average power ratio (PAPR). The basic DPA is based on a two-way structure where the carrier and peaking amplifiers are configured using two transistors having the same output power capacity [1]-[3]. The two-way symmetric DPA has an efficiency peak at the 6 dB OBO level.

The growing demand for a higher data rate has led to an increase in the PAPR of the modulated signals, which requires an operation with a larger OBO for the PA. Accordingly, an asymmetric DPA with a peaking amplifier of a larger power capacity has been proposed [4]-[5]. By obtaining more output power from the peaking amplifier, the peak efficiency point can be backed off by more than 6 dB. In addition, three-way DPA structures composed of one carrier and two peaking amplifiers have been proposed [6]. Since the output power from the two peaking amplifiers is higher than that from the carrier amplifier, the OBO level can be extended. Alternatively, to further extend the OBO, three-stage DPAs have been proposed [7]-[8]. Contrary to the three-way DPA structures where all peaking amplifiers are turned on at the same time, the three-stage DPA aligns the gate bias voltages to have different turn-on transitions of two peaking amplifiers. The different structures with different turn-on transitions of the three-stage DPA can create three peak efficiency points to have improved efficiency at the power transition region and an extended OBO level. However, since three-way or three-stage DPAs have three parallel paths, they could lower power gain due to three-way power splitting at the input compared to the two-way DPAs.

This paper presents a multi-mode Doherty power amplifier (M-DPA) GaN MMIC using four parallel amplifiers to have either 6 or 12 dB OBO level according to the mode selection. In 2C2P mode, it operates with two carrier and two peaking amplifiers for 6 dB OBO. In 1C3P mode, it operates with one carrier and three peaking amplifiers for 12 dB OBO. The proposed DPA can selectively optimize the performances between efficiency and gain. At a low average output power, the efficiency can be maximized using the 1C3P mode with 12 dB OBO. However, since the 1C3P mode has low gain characteristics, it can increase the power consumption of the drive amplifier at a high average output power. At a high average output power, the 2C2P mode with 6 dB OBO can be selected instead and using its high gain characteristic, it can reduce the burden of the drive amplifier.

II. Proposed M-DPA

A. M-DPA with four amplifiers

Fig. 1 shows (a) operational diagram and (b) fundamental current profile for the 2C2P mode. Four current sources (I_{1-4}) represent the four amplifiers with the same maximum currents, which means that the output power capacities of the four amplifiers are the same. For different current profiles of the four current sources according to the input signal, different modes of load modulation can be obtained. I_1 and I_2 are combined using current combiner (CC1), while I_3 and I_4 are combined using CC2. The power from the CC1 and CC2 is combined using the voltage combiner (VC). The CC and VC have quarter-wave transmission lines (TLs) whose characteristic impedances are R_0 and R_0/2, respectively. The load resistance is R_0. The phases of I_{1-4} should be set as 0°, -90°, 90°, and 0°, respectively.

In 2C2P mode, I_1 and I_3 represent the carrier amplifiers, while I_2 and I_4 represent the peaking amplifiers that start to turn on at $V_{in,nor}$ of 0.5. In the low power region where $V_{in,nor}$ ranges from 0 to 0.5, only the carrier amplifiers are turned on. The optimum load impedance of each amplifier at the peak output power is R_0. Therefore, Z_1 and Z_3 are $2R_0$,

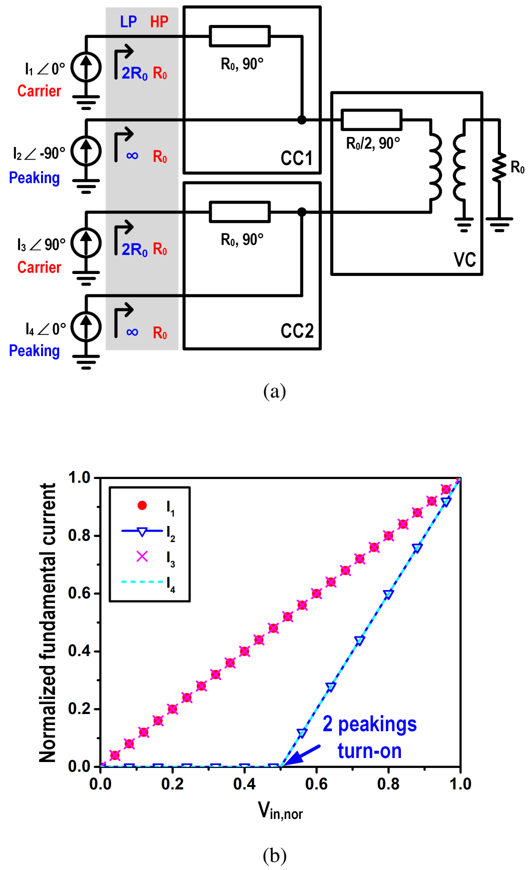

Fig. 1. (a) operational diagrams and (b) fundamental current profile for the 2C2P mode.

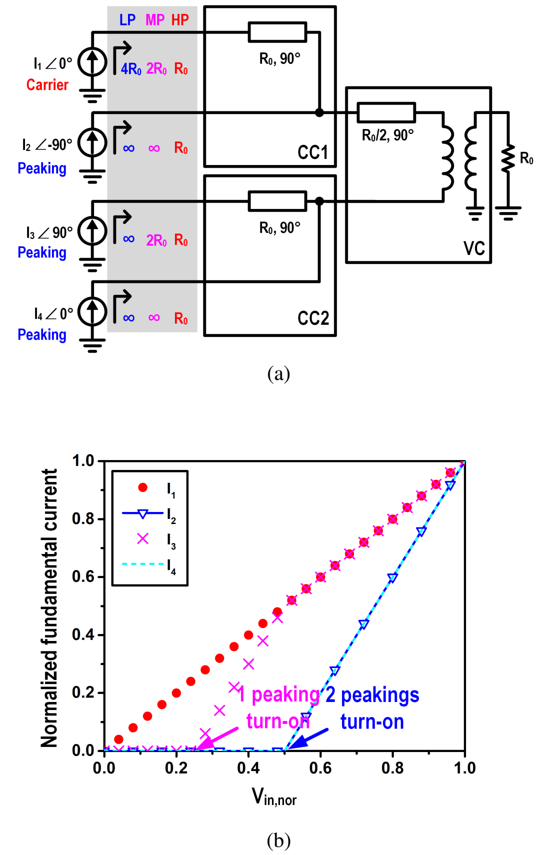

Fig. 2. (a) operational diagrams and (b) fundamental current profile for the 1C3P mode.

while Z_2 and Z_4 are ∞. At the peak power level where $V_{in,nor}$ is 1, the carrier and peaking amplifiers have peak fundamental currents. Therefore, all Z_{1-4} become R_0. As the input power increases from the low power to peak power level, just as in the conventional two-way DPA, the load impedances of the carrier and peaking amplifiers are modulated from $2R_0$ to R_0 and from ∞ to R_0, respectively.

Fig. 2 shows (a) operational diagram and (b) fundamental current profile for the 1C3P mode. For 1C3P mode, I_3 is turned on from $V_{in,nor}$ of 0.25, while I_2 and I_4 are turned on from $V_{in,nor}$ of 0.5. In the low power region, only the carrier amplifier is turned on. The output impedance of the peaking amplifier from the lower port of the output transformer (TF) becomes ideally zero. Then, Z_1 becomes $4R_0$ using two quarter-wave TLs at CC1 and VC. For $V_{in,nor}$ from 0.25 to 0.5, since I_2 and I_4 are still turned off, the VC provides the load modulation as well. I_3 becomes the same as I_1 of the carrier amplifier at $V_{in,nor}$ of 0.5. Therefore, Z_1 and Z_3 are $2R_0$, while Z_2 and Z_4 are ∞. Then, two other peaking amplifiers, I_2 and I_4, start to turn on from $V_{in,nor}$ of 0.5 and all the 4 amplifiers have the maximum current at $V_{in,nor}$ of 1. Therefore, Z_{1-4} all become R_0. As results, for the 2C2P mode, the second efficiency peak is obtained at a $V_{in,nor}$ of 0.5 for 6 dB OBO, while for the 1C3P mode, the second and third efficiency peaks are obtained at a $V_{in,nor}$ of 0.5 and 0.25, respectively.

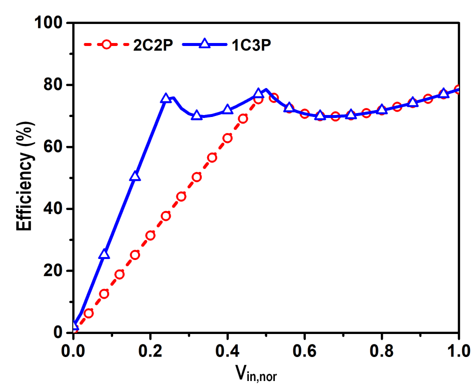

Fig. 3. Ideal efficiency curves of the proposed M-DPA for 2C2P and 1C3P modes.

Fig. 3 shows the ideal efficiency curves of the M-DPA for the multiple operation modes. For the 2C2P mode, the second efficiency peak is obtained at a $V_{in,nor}$ of 0.5 for 6 dB OBO. For the 1C3P mode, the second and third efficiency peaks are obtained at a $V_{in,nor}$ of 0.25 and 0.5, respectively.

B. Design of the M-DPA

Fig. 4 shows a schematic of the designed M-DPA MMIC based on the lumped components for 3.3-3.6 GHz. The

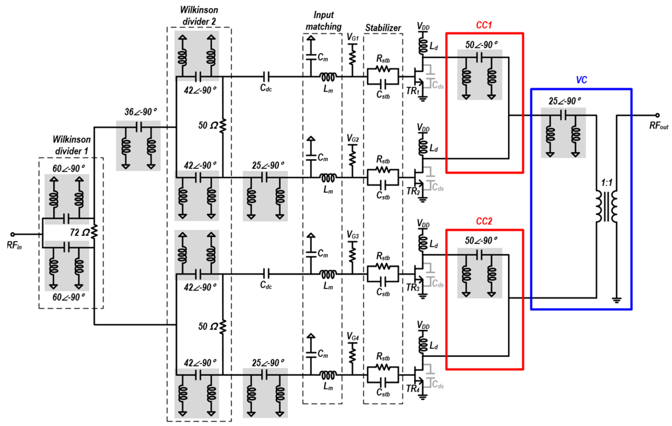

Fig. 4. Schematic of the designed M-DPA using four amplifiers and lumped components.

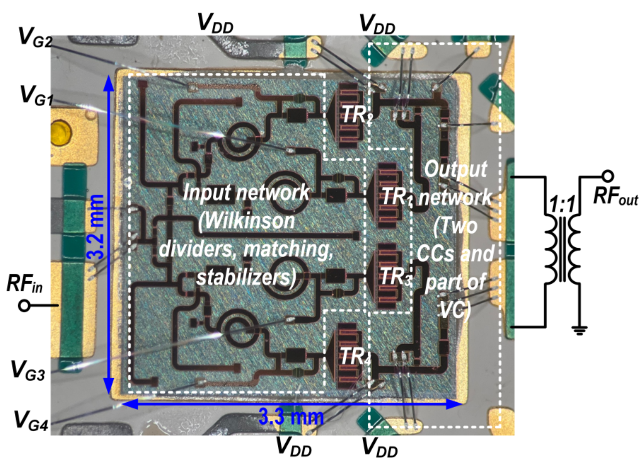

Fig. 5. Micrograph of the fabricated M-DPA MMIC using 0.25 μm GaN-HEMT process.

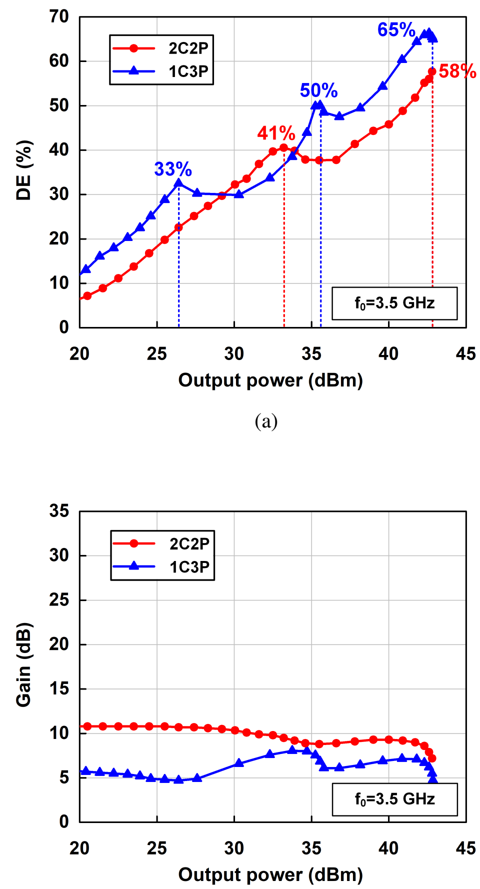

(a)

(b)

Fig. 6. Measured (a) DE and (b) power gain using 3.5 GHz 1-tone CW for 2C2P and 1C3P modes

load network (LN) consists of two CCs and one VC. The quarter-wave TLs for the input and load networks were designed using a high-pass L-C-L network. The input impedance is matched to 25 Ω using the low-pass input matching circuit based on L_m and C_m. RF_{in} is divided into two paths for an impedance of 36 Ω by the Wilkinson divider 1. Then, the signals are divided into four paths for an impedance of 25 Ω by the Wilkinson divider 2. The designed M-DPA can be simplified by merging the components in parallel at the same node. For the LN, 10 inductors at the design before simplification were reduced to 6 inductors. To minimize the loss and size of the LN, some inductors are realized using high-Q bond wires. The TF in the VC is designed on the evaluation board. For the input network, 18 inductors can be reduced to 5 inductors after simplification.

III. Implementation and Experimental Results

Fig. 5 shows the micrograph of the implemented M-DPA MMIC. The MMIC was fabricated using Win-semiconductor's 0.25 μm GaN-HEMT process and has a size of 3.3x3.2 mm^2. The supply voltage (V_{DD}) was 28 V. Fig. 6 shows the measured (a) drain efficiency (DE) and (b) power gain using a 3.5 GHz CW signal. For the 2C2P mode, two efficiency peaks were obtained. DE of 58% and 41% were obtained at the first and second peak efficiency points, respectively. For the 1C3P mode, three efficiency peaks were observed. DEs of 65%, 50%, and 33% were obtained at the first, second, and third efficiency peaks, respectively. Compared to the 1C3P mode, relatively higher power gain was obtained for the 2C2P mode.

Fig. 7 shows the measured DE and gain for the frequency band of 3.3-3.6 GHz using the 5G NR signal with a signal bandwidth of 100 MHz and a PAPR of 7.86 dB. For the 2C2P and 1C3P modes, DEs of 35.1-37.6% and 44.1-46.8% at an average output power of 37.0 dBm were obtained, respectively. For the 1C3P mode, DE of 27.0-35.2% at a relatively low average output power of 31.0 dBm was achieved, which is higher than 22.6-33.3% from the 2C2P mode at the same output power. However, the 2C2P mode has a relatively higher power gain compared to the 1C3P mode. Measurement results of this work are summarized in Table 1.

IV. Conclusion

This paper presents a GaN-HEMT M-DPA MMIC using four parallel amplifiers for sub-6 GHz 5G application. Either

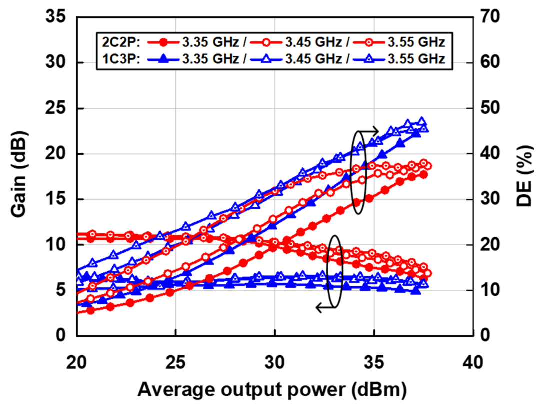

Fig. 7. Measured DE and gain for the frequency band of 3.3-3.6 GHz using the 5G NR signal.

Table 1. Performance summary and comparison to the previously reported GaN DPA MMICs for the sub-6 GHz 5G application.

Ref.	**This work**		[1] 2022 TMTT	[2] 2022 JSSC	[3] 2019 MWCL
Freq. (GHz)	**3.3-3.6**		3.35-3.6 / 4.8-5.8	4.1-5.6	3.3-3.8 / 5.8
Modulation	**NR 100 M**		NR 100 M	NR 100 M	- 40 M
Mode	**2C2P**	**1C3P**	1C1P	1C1P	1C1P
P_{sat} (dBm)	**42.6-43.0**	**42.0-42.9**	43.8-44.7 / 44.4-44.8	38.4-39.5	41.8-42.6 / 41.0
DE at 6 dB OBO (%)	**34.7-39.0**	**38.1-47.5**	41.0-46.0 / 41.5-47.0	38.5-46.5	42.0-51.0 / 29.0*
DE at 12 dB OBO (%)	**18.3-33.1**	**22.1-33.7**	23.0-27.0* / 23.0-30.0*	17.0-19.0*	23.0* / 15.0*
P_{avg} (dBm)	**37.0**	**31.0**	36.1-37.0	32.5	32.5
DE at P_{avg} (%)	**35.1-37.6**	**27.0-35.2**	34.5-40.0	38.6-42.3	-

*Graphically estimated

2C2P or 1C3P mode can be selected by arranging the turn-on transition of four parallel amplifiers according to the input power level. For the 2C2P mode, four amplifiers are configured with two carrier and two peaking amplifiers for 6 dB OBO. On the other hand, the 1C3P mode has one carrier and three peaking amplifiers for 12 dB OBO. For the frequency band of 3.3-3.6 GHz, the 2C2P and 1C3P operations were verified using a CW signal and the 5G NR modulated signal.

References

[1] G. Lv *et al.*, "A fully integrated 3.5-/4.9-GHz dual-band GaN MMIC Doherty power amplifier based on multi-resonant circuits," *IEEE Trans. Microw. Theory Techn.*, vol. 70, no. 1, pp. 416–431, Jan. 2022.

[2] J. Pang *et al.*, "Broadband GaN MMIC Doherty power amplifier using continuous-mode combining for 5G sub-6 GHz applications," *IEEE J. Solid-State Circuits*, vol. 57, no. 7, pp. 2143–2154, Jul. 2022.

[3] G. Lv, W. Chen, X. Liu, and Z. Feng, "A dual-band GaN MMIC power amplifier with hybrid operating modes for 5G application," *IEEE Microw. Wireless Compon. Lett.*, vol. 29, no. 3, pp. 228–230, Mar. 2019.

[4] H. Oh *et al.*, "Doherty power amplifier based on the fundamental current ratio for asymmetric cells ," *IEEE Trans. Microw. Theory Techn.*, vol. 65, no. 11, pp. 4190–4197, Nov. 2017.

[5] W. Choi, H. Kang, H. Oh, K. C. Hwang, K.-Y. Lee, and Y. Yang, "Doherty power amplifier based on asymmetric cells with complex combining load," *IEEE Trans. Microw. Theory Techn.*, vol. 69, no. 4, pp. 2336–2344, Apr. 2021.

[6] H. Kang *et al.*, "Symmetric three-way Doherty power amplifier for high efficiency and linearity," *IEEE Trans. Circuits Syst. II, Express Briefs*, vol. 64, no. 8, pp. 862–866, Aug. 2017.

[7] Y. Xu, J. Pang, X. Wang, and A. Zhu, "Three-stage load modulated power amplifier with efficiency enhancement at power back-off," *IEEE Trans. Microw. Theory Techn.*, vol. 69, no. 6, pp. 3107–3119, Jun. 2021.

[8] H. Zhou *et al.*, "A generic theory for design of efficient three-stage Doherty power amplifiers," *IEEE Trans. Microw. Theory Techn.*, vol. 70, no. 2, pp. 1242–1253, Feb. 2022.

[9] N. B. Vangipurapu, H. Lyu, Y. Cao and K. Chen, "Intrinsically mode-reconfigurable load-modulation power amplifier leveraging transistor's analog-digital duality," in *IEEE MTT-S Int. Microw. Symp. Dig.*, Jun. 2022, pp. 418–421.

[10] V. Vorapipat, C. S. Levy, and P. M. Asbeck, "Voltage mode Doherty power amplifier," *IEEE J. Solid-State Circuits*, vol. 52, no. 5, pp. 1295–1304, May 2017.

[11] H. Oh *et al.*, "2.8-3.8 GHz broadband InGaP/GaAs HBT Doherty power amplifier IC for 5G new radio handset," in *IEEE MTT-S Int. Microw. Symp. Dig.*, Jun. 2022, pp. 849–852.

[12] A. Jundi and S. Boumaiza, "A series-connected-load Doherty power amplifier with push–pull main and auxiliary amplifiers for base station applications," *IEEE Trans. Microw. Theory Techn.*, vol. 68, no. 2, pp. 796–807, Feb. 2020.